

2019-02

# Contrasting responses of stomatal conductance and photosynthetic capacity to warming and elevated CO<sub>2</sub> in the tropical tree species *Alchornea glandulosa* under heatwave conditions

Fauset, S

<http://hdl.handle.net/10026.1/12897>

---

10.1016/j.envexpbot.2018.10.030

Environmental and Experimental Botany

Elsevier

---

*All content in PEARL is protected by copyright law. Author manuscripts are made available in accordance with publisher policies. Please cite only the published version using the details provided on the item record or document. In the absence of an open licence (e.g. Creative Commons), permissions for further reuse of content should be sought from the publisher or author.*

1 Contrasting responses of stomatal conductance and photosynthetic capacity to  
2 warming and elevated CO<sub>2</sub> in the tropical tree species *Alchornea glandulosa* under  
3 heatwave conditions

4

5 Sophie Fauset<sup>1\*</sup>, Lauana Oliveira<sup>2</sup>, Marcos Buckeridge<sup>2</sup>, Christine H. Foyer<sup>3</sup>, David  
6 Galbraith<sup>1</sup>, Rakesh Tiwari<sup>1</sup>, Manuel Gloor<sup>1</sup>

7

8 <sup>1</sup> School of Geography, University of Leeds, Leeds, LS2 9JT, UK

9 <sup>2</sup> Instituto de Biociências, Universidade de São Paulo, São Paulo, 05508-090, Brazil

10 <sup>3</sup> Centre for Plant Sciences, University of Leeds, Leeds, LS2 9JT, UK

11 \* Correspondence author, [Sophie.fauset@plymouth.ac.uk](mailto:Sophie.fauset@plymouth.ac.uk), present address School of  
12 Geography, Earth, and Environmental Sciences, University of Plymouth, Plymouth,  
13 PL4 8AA, UK

14

## 15 **Abstract**

16

17 Factorial experiments of combined warming and elevated CO<sub>2</sub> are rarely performed  
18 but essential for our understanding of plant physiological responses to climate change.  
19 Studies of tropical species are particularly lacking, hence we grew juvenile trees of  
20 *Alchornea glandulosa* under conditions of elevated temperature (+1.5°C, eT) and  
21 elevated CO<sub>2</sub> (+400ppm, eC) in a factorial open top chamber experiment. We  
22 addressed three questions: i) To what extent does stomatal conductance ( $g_s$ ) reduce  
23 with eT and eC treatments?; ii) Is there an interactive effect of eT and eC on  $g_s$ ?; iii)  
24 Does reduced  $g_s$  as a result of eT and/or eC cause an increase in leaf temperature?; iv)  
25 Do the photosynthetic temperature optima ( $T_{opt}$ ) and temperature response of

26 photosynthetic capacities ( $V_{cmax}$ ,  $J_{max}$ ) shift with higher growth temperatures? The  
27 experiment was performed during an anomalously hot period, including a heatwave  
28 during the acclimation period. Our key findings are that: 1) the eT treatment reduced  
29  $g_s$  more than the eC treatment, 2) reduced  $g_s$  caused an increase in leaf temperatures,  
30 and 3) net photosynthesis and photosynthetic capacities showed very high  
31 temperature tolerances with no evidence for acclimation to the eT treatment. Our  
32 results suggest that *A. glandulosa* may be able to cope with increases in air  
33 temperatures, however reductions in  $g_s$  may cause higher leaf temperatures beyond  
34 those induced by an air temperature rise over the coming century.

35

36 Keywords: photosynthesis, climate change, factorial experiment, tropical forest,  
37 warming, carbon dioxide, leaf temperature,  $v_{cmax}$ ,  $j_{max}$ , temperature optima, open  
38 top chamber, photosynthetic capacity

39

## 40 **1. Introduction**

41

42 Global atmospheric CO<sub>2</sub> concentrations are increasing, as are air temperatures, with  
43 both patterns expected to continue in the coming decades. Plants are a critical part of  
44 global biogeochemical cycles, at the interface of the atmosphere and the land surface,  
45 with forests storing 65% of terrestrial aboveground biomass (Liu et al., 2015). Plants  
46 respond to environmental stimuli, with long-term adaptation and short-term  
47 acclimation to changes in light, temperature and other conditions. Photosynthesis,  
48 evapotranspiration, and respiration are the primary functions of leaves. Our  
49 understanding of leaf-level physiology is used to drive vegetation and land surface  
50 models, and hence to project future climate. Experimental research on the responses

51 of forests to elevated CO<sub>2</sub> has been heavily focussed on temperate ecosystems  
52 (Leakey et al. 2012) despite tropical forests stocking more carbon than temperate and  
53 boreal forests combined (Pan et al. 2011). Similarly, there are very few studies of  
54 thermal acclimation on tropical species (Dusenge & Way 2017). Although  
55 temperature increases in the tropics are predicted to be smaller than in other regions  
56 (e.g. boreal zone, Collins et al. 2013), tropical forests experience much lower diurnal  
57 and seasonal variation in temperature than temperate or boreal forests, and over  
58 geological time have experienced a relatively stable climate, potentially reducing the  
59 acclimation potential of tropical tree species (Janzen 1967, Dusenge & Way 2017).  
60 Investigating the responses of tropical tree species to temperature and CO<sub>2</sub> is  
61 therefore a research priority.

62

63 Increasing air temperatures and atmospheric CO<sub>2</sub> concentrations lead to changes in  
64 stomatal conductance ( $g_s$ ) over short and long timescales (Way et al., 2015). In the  
65 short-term (instantaneous responses), increasing air temperatures typically lead to a  
66 reduction in  $g_s$  (Way et al., 2015, Slot & Winter 2017a) due to stomatal closure with  
67 increasing vapour pressure deficit ( $D$ ), which prevents excessive water loss under  
68 high evaporative demand. At very high temperatures,  $g_s$  may actually increase in  
69 order to avoid reaching dangerously high leaf temperatures (Slot et al., 2016, Slot &  
70 Winter 2017b, Urban et al., 2017, Drake et al., 2018). Evidence of acclimation of  $g_s$  to  
71 higher temperatures in trees over the long-term is varied, however some species show  
72 declines (Way et al., 2015). The instantaneous response of  $g_s$  to increased CO<sub>2</sub> is to  
73 decrease, which reduces water loss while maintaining a high internal leaf CO<sub>2</sub>  
74 concentration ( $c_i$ ) (Gaastra, 1959). Similarly, under long-term CO<sub>2</sub> enrichment,  $g_s$   
75 reduces. Such declines in  $g_s$  may increase leaf temperature ( $T_L$ ) through reduced

76 evaporative cooling (under increased air temperatures, reduced evaporative cooling  
77 would also depend on the extent of increased  $D$ , Oren et al. 1999). Higher  $T_L$  could  
78 push leaves beyond their photosynthetic temperature optima ( $T_{opt}$ ) (Doughty &  
79 Goulden 2008, Slot & Winter 2017c), and potentially above their physiological  
80 temperature tolerances (O’Sullivan et al., 2017) causing permanent leaf damage under  
81 extreme heat conditions (Warren et al., 2011). While the response of  $g_s$  to combined  
82 elevated  $CO_2$  (eC) and temperature (eT) has rarely been tested (Way et al., 2015,  
83 Becklin et al., 2017), experiments on eucalyptus (Ghannoum et al., 2010), douglas-fir  
84 (Lewis et al., 2002) and loblolly pine (Wertin et al. 2010) showed little interactive  
85 effect; if the two do interact and lead to even greater decreases in  $g_s$ , this would  
86 increase  $T_L$  further.

87

88 Long-term increasing air temperatures and  $CO_2$  concentrations are also predicted to  
89 induce changes in net photosynthesis, both directly by impacting biochemical  
90 processes and indirectly through changes in  $g_s$ . Increases in  $T_L$  either directly from  
91 increased air temperatures or indirectly from a long-term reduction in  $g_s$  could shift  
92 the leaf beyond  $T_{opt}$ , leading to reductions in photosynthesis. Some experimental  
93 studies have shown partial photosynthetic acclimation to increasing temperatures  
94 through increases in  $T_{opt}$  (Yamori et al., 2014, Slot & Winter 2017b), which could  
95 occur due to alterations in membrane fluidity, expression of heat shock proteins, and  
96 production of greater quantities of Rubisco activase or a heat-stable Rubisco activase  
97 (Yamori et al. 2014). These changes would lead to altered temperature responses of  
98 the photosynthetic capacities  $V_{cmax}$  (maximum rate of carboxylation) and  $J_{max}$   
99 (maximum rate of electron transport). A recent study of four tropical tree species  
100 showed that  $g_s$  rather than  $V_{cmax}$  or  $J_{max}$  limited net photosynthesis beyond  $T_{opt}$  (Slot &

101 Winter 2017a), and hence a change to the temperature (or  $D$ ) response of  $g_s$  could also  
102 be important for shifts in  $T_{opt}$ . Photosynthetic capacities are also influenced by growth  
103  $CO_2$  concentrations. Under high  $CO_2$ , Rubisco concentrations typically reduce and  
104 hence  $V_{cmax}$  declines (Way et al. 2015). Decreases in  $g_s$  (as a consequence of increased  
105 air temperature or  $CO_2$ ) lead to reduced  $c_i$  which can reduce assimilation. Under high  
106  $CO_2$  concentrations, this effect could be limited if  $c_i$  remains above the Rubisco  
107 limited portion of the  $A-c_i$  curve, however the downregulation of  $V_{cmax}$  commonly  
108 observed results in plants still being Rubisco limited even at high  $CO_2$  (Ainsworth &  
109 Rogers 2007) and hence reduced  $g_s$  could still reduce assimilation (Way et al., 2015).

110

111 The effect of decreased conductance on  $T_L$  is well understood biophysically (Jones  
112 1992) and is expected to influence  $T_L$  under elevated  $CO_2$  (Drake et al. 1997), as has  
113 been shown in a small number of experiments (e.g. Siebke et al. 2002, Sigut et al.  
114 2015). However, this effect has not been investigated in any tropical species.

115 Furthermore, because  $T_L$  and, to a lesser extent,  $g_s$  show high temporal variation with  
116 changing microclimate (e.g. Fauset et al., 2018), to fully investigate the effect of  
117 altered  $g_s$  as a response to elevated temperature and  $CO_2$  it is necessary to measure  $T_L$   
118 and microclimate with a high temporal resolution.

119

120 In this study, we address the following questions using a factorial eT x eC open top  
121 chamber experiment with juveniles of tropical tree species *Alchornea glandulosa*  
122 (Poepp. & Endl) (Euphorbiaceae): i) To what extent does  $g_s$  reduce with elevated  
123 temperature (eT) and elevated  $CO_2$  (eC) treatments?; ii) Is there an interactive effect  
124 of eT and eC on  $g_s$ ?; iii) Does reduced  $g_s$  as a result of eT and/or eC cause an increase  
125 in  $T_L$ ?; iv) Do the photosynthetic temperature optima ( $T_{opt}$ ) and temperature response

126 of photosynthetic capacities ( $V_{cmax}$ ,  $J_{max}$ ) shift with higher leaf temperatures? *A.*  
127 *glandulosa* is a pioneer species often found, but not restricted to, riverine  
128 environments (Pascotto 2006), distributed in the Atlantic forest, western  
129 Amazon/Andes and central America (GBIF Secretariat 2017), with over 100,000,000  
130 individual trees estimated to occur in the Amazon (ter Steege et al., 2013). It is  
131 utilized as a timber species, produces medicinal compounds and is used for  
132 reforestation in the Atlantic forest region. The fruits of this tree are an important food  
133 source for birds (Pascotto 2006). This species was also selected because leaf  
134 temperature and stomatal conductance field data for congeneric species *Alchornea*  
135 *triplinervia* were available from the Atlantic forest (Fauset et al., 2018).

136

## 137 **2. Methods**

138

### 139 *2.1 Experimental setup*

140

141 The study was carried out at the University of São Paulo from February to March  
142 2017 (23.56° S, 46.73° W, elevation 760 m). *Alchornea glandulosa* seedlings were  
143 sourced from a local plant nursery where they were germinated in shade houses  
144 before growing for 12 months outside.

145

146 The seedlings were moved to the glasshouse in September 2016 and in November  
147 transferred into containers (4l PVC pots with one plant per plot). Hoagland fertilizer  
148 solution was added every 2 weeks. The experiment was conducted using four  
149 polycarbonate open top chambers (OTCs) with modifications (Aidar et al., 2002)  
150 located within the glass house. The four treatments were: i) control (aTaC), ii)

151 elevated CO<sub>2</sub> (ambient temperature, 800 ppm CO<sub>2</sub>, aTeC), iii) elevated temperature  
152 (temperature 1.5°C above ambient, ambient CO<sub>2</sub>, eTaC), and iv) elevated CO<sub>2</sub> and  
153 elevated temperature (temperature 1.5°C above ambient, 800 ppm CO<sub>2</sub>, eTeC). Each  
154 chamber had an air inlet at the base with a fan, and a spiral heater and/or CO<sub>2</sub> gas inlet  
155 was present depending on the treatment (Figure S1). Temperature within the chamber  
156 was thermostatically controlled using RICS software (Remote Integrated Control  
157 System) with the heater switched on or off to maintain a higher temperature than the  
158 unheated chambers. No attempt was made to control for differences in  $D$  due to  
159 temperature treatments as increases in temperature would be associated with increases  
160 in  $D$  under future conditions assuming no change in relative humidity. CO<sub>2</sub> was  
161 passively added to the eC treatments through the use of pressurized CO<sub>2</sub> cylinders.  
162 The CO<sub>2</sub> concentrations of the eC chambers was monitored daily and the flow into the  
163 chambers altered at a valve if the concentration decreased. Further details of the  
164 experimental design can be found in Aidar et al., 2002 and de Souza et al. (2008). Ten  
165 seedlings were placed into each chamber on 1 February 2017 and allowed to  
166 acclimate for one month before measurements began. Vertical height of each seedling  
167 was recorded prior to placement in the OTCs, and placement of seedlings into OTCs  
168 was stratified to ensure an even spread of vertical heights.

169

## 170 *2.2 Microclimate measurements*

171

172 Within each OTC air temperature ( $T_A$ ), relative humidity ( $h$ ) and CO<sub>2</sub> concentration  
173 were measured at 5 min intervals (Testo 535, Testo Inc., Flanders, NJ, USA). An  
174 additional  $T_A$  sensor (107 thermistor, Campbell Scientific) recorded air temperature  
175 every 10 s inside each chamber.

176

## 177 2.3 Physiological Measurements

178

### 179 2.3.1 Leaf temperature and leaf surface PAR

180 The eight healthiest of the ten seedlings in each chamber were selected for  
181 measurement of leaf temperature. On each selected seedling, one fully expanded  
182 healthy leaf was chosen (typically the fourth or fifth newest leaf). These leaves were  
183 formed inside the glass house but prior to movement of the seedling into the OTCs.  
184 Prior to selection, we verified that the leaves were photosynthetically active. A two-  
185 junction thermocouple (copper-constantan, type T) that measured leaf-to-air  
186 temperature difference ( $\Delta T_L$ ) was attached to the abaxial surface of each sample leaf  
187 using a piece of breathable tape (Transpore, 3M, St. Paul MN) following the protocol  
188 of Fauset et al. (2018). One thermocouple was used per leaf. Absolute leaf  
189 temperatures ( $T_L$ ) were calculated from  $\Delta T_L$  and  $T_A$  in each chamber measured by the  
190 thermistors. A photosynthetically active radiation (PAR) sensor built to the  
191 specification of Fielder & Comeau (2000) was positioned adjacent to each sample leaf  
192 at the same angle and orientation. PAR sensors were calibrated against a quantum  
193 sensor (LightScout, Spectrum Technologies, Aurora, Illinois).  $\Delta T_L$  and leaf surface  
194 PAR were monitored continuously at 10 s measuring frequency between 24 February  
195 – 15 March 2017 using two CR800 data loggers and two AM16/32 multiplexers  
196 (Campbell Scientific). Measurements of some leaves were terminated between 10 and  
197 15 March. See Fauset et al. (2017, 2018) for further details of these sensors.

198

### 199 2.3.2 Stomatal Conductance

200 Stomatal conductance ( $g_s$ ) of each leaf temperature sample leaf was measured under  
201 growth conditions inside the chambers on 19 occasions over six days (including four  
202 days where  $g_s$  of each leaf was measured at least four times, 28 February – 7 March  
203 2017) using an SC-1 porometer (Decagon). For each time point, two measurements of  
204  $g_s$  were recorded, one from either side of the midrib, and the mean value was used for  
205 analysis.

206

### 207 2.3.3 Photosynthetic measurements

208 The temperature response of photosynthesis was measured using a LI-COR 6400XT  
209 portable photosynthesis measurement system (LI-COR, Nebraska). Data were  
210 collected from 10 – 18 March 2018. Light response curves on 3 leaves showed  
211 saturating photosynthesis at  $800 \mu\text{mol m}^{-2} \text{s}^{-1}$  PAR (Figure S2), hence all  
212 measurements were taken at  $800 \mu\text{mol m}^{-2} \text{s}^{-1}$  PAR using the standard red-blue LED  
213 light source. Note that the glasshouse roof was made of a diffusing plastic which  
214 reduced the incoming PAR by c. 60 % compared with the outside, and leaf level PAR  
215 reached c.  $800 \mu\text{mol m}^{-2} \text{s}^{-1}$ , varying with leaf angle and orientation. Three seedlings  
216 from each OTC were selected for photosynthesis measurements and the leaf  
217 measurements were performed on the same leaf as leaf temperature monitoring. Two  
218 sets of measurements were made, net photosynthesis-temperature curves ( $A-T_L$  curves  
219 where net photosynthesis at saturating light intensity is measured at different  
220 temperatures), and  $A-c_i$  curves (where net photosynthesis at saturating light intensity  
221 is measured at different  $\text{CO}_2$  concentrations) at three different temperatures.  $A-T$   
222 curves were run with the  $\text{CO}_2$  concentration of the relevant OTC (either 400 or 800  
223 ppm  $\text{CO}_2$ ) and assimilation was measured at leaf chamber temperatures of 20, 25, 27,  
224 29, 31, 33, 35 and 40 °C, with 5 measurements recorded at each temperature after the

225 photosynthetic rate and  $g_s$  had stabilized. Measurements at 20, 30 and 35 °C were  
226 supplemented using the relevant measurements from the  $A-c_i$  curves.  $A-c_i$  curves used  
227 the following sequence of CO<sub>2</sub> concentrations (ppm); 400, 200, 100, 50, 400, 600,  
228 800, 1200, 1500, 2000.  $A-c_i$  curves were performed at three temperatures, 20, 30, and  
229 35 °C, and each curve was performed twice for each leaf on either side of the midrib.  
230 For all measurements,  $h$  was maintained as close as possible to 50 % using a  
231 combination of desiccant and adjusting the air flow rate; it was difficult to maintain  
232 this  $h$  at leaf temperatures above 37 °C (on average 46 %, minimum values were 40  
233 %). The temperature of the chamber was mostly controlled using the inbuilt  
234 temperature control system. In addition, for most of the measurements the sensor head  
235 was placed inside a specially designed temperature control chamber to enable better  
236 control of the chamber temperature (Yepes Mayorga 2010). The temperature control  
237 box was switched off during measurements but was used to aid the change of  
238 chamber temperature between measurements. Measurements were made at an  
239 atmospheric pressure in the greenhouse of 92.6 kPa.

240

#### 241 2.3.4 Plant growth

242 Vertical height (from soil surface) and number of leaves of each seedling was  
243 measured three times (1 and 21 February, and 16 March). On the latter two  
244 measurement days, the length of the seedling from the soil surface to the end of the  
245 longest branch was also recorded, and on 16 March the total plant length including all  
246 branches was recorded.

247

#### 248 2.4 Data analysis

249

250 Differences in microclimate between OTCs (air temperature, CO<sub>2</sub> concentration, *h*  
251 and *D*) were tested using ANOVA and Tukey post-hoc test.  
252  
253 The effects of the warming and the elevated CO<sub>2</sub> treatments on *g<sub>s</sub>* (porometer  
254 measurements pooled from all times of day) were tested using two-way ANOVA with  
255 a mixed effects model with leaf as a random factor to account for multiple  
256 measurements of the same leaves (function ‘lme’ of the R package nlme, Pinheiro et  
257 al. 2017). To investigate the response of *g<sub>s</sub>* to microclimate variables and under  
258 different treatments, all possible models of PAR and leaf-to-air vapour pressure  
259 deficit *D<sub>L</sub>* (where leaf temperature was taken from thermocouple data), with  
260 interactions with CO<sub>2</sub> treatment and warming treatment were compared using AIC to  
261 select the best model with the function ‘dredge’ in R package MuMIn (Bartoń 2017).  
262 Again, a linear mixed effect model with leaf as a random factor was used to account  
263 for multiple measurements of the same leaf/seedling. A quadratic effect of time was  
264 also included in the model to account for diurnal changes in *g<sub>s</sub>* not directly linked to  
265 PAR, temperature or *D<sub>L</sub>*. *R*<sup>2</sup> for mixed-effects models are given using as the marginal  
266 pseudo *R*<sup>2</sup> that accounts for fixed factors only rather than the conditional pseudo *R*<sup>2</sup>  
267 which also accounts for random effects (Nakagawa & Schielzeth 2013) unless  
268 otherwise stated; *R*<sup>2</sup> values for mixed effects models were calculated using the  
269 function provided in the R package MuMIn. We also estimated the *g<sub>l</sub>* parameter of  
270 the optimal stomatal conductance model (Medlyn et al. 2011, Lin et al. 2015) from  
271 the A-T<sub>L</sub> curve data collected with the LI-COR 6400.

272 
$$g_s = 1.6 \left( 1 + \frac{g_l}{\sqrt{D}} \right) \frac{A}{C_a}$$

273 where *C<sub>a</sub>* is the atmospheric CO<sub>2</sub> concentration in the leaf chamber. The model was fit  
274 for each leaf, and the *g<sub>l</sub>* parameter was compared between chambers using ANOVA.

275

276 Because leaf temperatures are strongly influenced by microclimate (Jones 1993,  
277 Fauset et al. 2018), to assess the influence of treatment on  $T_L$  it is necessary to  
278 compare  $T_L$  within microclimatic envelopes. We subsetted the data into envelopes  
279 based on leaf-level PAR, chamber air temperature and  $D$ . The data was split into low  
280 ( $100 - 200 \mu\text{mol m}^{-2} \text{s}^{-1}$ ), medium ( $400 - 500 \mu\text{mol m}^{-2} \text{s}^{-1}$ ) and high ( $700 - 800 \mu\text{mol}$   
281  $\text{m}^{-2} \text{s}^{-1}$ ) PAR, and low ( $28 - 30 \text{ }^\circ\text{C}$ , 1 - 2 kPa), medium ( $33 - 35 \text{ }^\circ\text{C}$ , 2 - 3 kPa), and  
282 high ( $38 - 40 \text{ }^\circ\text{C}$ , 3 - 4 kPa) air temperature and  $D$ . An unanticipated effect of the  
283 switching on and off of the heater in the warmed chambers was a cycle in leaf  
284 temperature. This was particularly clear at night, but also occurred during the day.  
285 When the heater was switched on, the  $\Delta T_L$  became more negative as the air heated  
286 faster than the leaf (Figure S3). The  $\Delta T_L$  then rose to reach an equilibrium  
287 temperature. Because of this cycle in the  $\Delta T_L$  data, it was not possible to compare leaf  
288 temperatures directly between the ambient and heated chambers, and hence direct  
289 comparisons on  $\Delta T_L$  were only made between  $\text{CO}_2$  treatments within temperature  
290 treatments.

291

292 The temperature response of photosynthesis is typically modelled as a parabolic curve  
293 which provides a  $T_{opt}$  parameter (e.g. Robakowski et al. 2012). However, as no  
294 evidence of a decline of  $A$  with increasing  $T_L$  was found (see section 3.4), we could  
295 not use the parabolic curve to find  $T_{opt}$  (Fig. S4) which was beyond the range of our  
296 measurements. Hence, a linear mixed effect model with leaf as a random factor was  
297 used to test the relationship between  $A$  and  $T_L$ . As for stomatal conductance we  
298 selected the best model based on AIC from all possible models, here including  $T_L$  as a  
299 continuous fixed effect and interactions with  $\text{CO}_2$  treatment and warming treatment.

300

301  $V_{cmax}$  and  $J_{max}$  were estimated for each leaf and each temperature from the  $A-c_i$  curve  
302 using the Farquhar-von Caemmerer-Berry model using the R package plantecophys  
303 (Duursma 2015). For some curves (six for  $J_{max}$  and one for  $V_{cmax}$ , all at 20 °C), the  
304 parameters could not be adequately estimated and estimates were not used. Of the  
305 remaining fits, the root mean square error ranged 0.18 – 1.57  $\mu\text{mol m}^{-2} \text{s}^{-1}$ . The  
306 temperature responses of  $V_{cmax}$  and  $J_{max}$  were modelled using the Arrhenius function  
307 (Medlyn et al. 2002)

308

309 
$$f(T_k) = k_{25} \cdot \exp\left(\frac{E_a(T_k - 298)}{(298RT_k)}\right)$$

310

311 where  $k_{25}$  is the value of  $V_{cmax}$  or  $J_{max}$  at 25 °C,  $E_a$  is the activation energy ( $\text{kJ mol}^{-1}$ ),  
312  $T_k$  is the leaf temperature ( $^{\circ}\text{K}$ ) and R is the universal gas constant ( $8.314 \text{ J mol}^{-1} \text{ K}^{-1}$ ).  
313 The parameters were fit using non-linear least squares (R function nls). This function  
314 was fit separately for each chamber, and significant differences in parameter estimates  
315 were tested by comparing the 95 % confidence intervals (following Varhammar et al.  
316 2015). A peaked Arrhenius function was not used as the data did not show a decline  
317 in  $V_{cmax}$  or  $J_{max}$  at high temperatures.

318

### 319 **3. Results**

320

#### 321 *3.1 Microclimate over the study period*

322

323 The experimental period coincided with an anomalously hot summer in São Paulo  
324 city including a 4 day heatwave (Figure 1). Using the definition of a heatwave from

325 Russo et al. (2015) as  $\geq 3$  consecutive days where the maximum temperature exceeds  
326 the 90<sup>th</sup> percentile of maximum temperatures from a monthly window for the period  
327 1981-2010, and climate data for the Mirante de Santana weather station (INMET), a  
328 four day heatwave period occurred (maximum temperatures above 32.3 °C) in mid-  
329 February (Figure 1, Figure S5). The heatwave occurred during the acclimation period  
330 but before the initiation of data collection. During this time the maximum daily air  
331 temperatures within the OTCs exceeded 45 °C (Figure 1).

332

333 Mean daily temperatures within the OTCs over the acclimation and measurement  
334 periods were significantly different between chambers ( $F = 5.4$ ,  $P = 0.001$ , ANOVA,  
335 Figure 2a). Temperatures were significantly lower in the aTeC treatment ( $28.8 \pm 2.3$   
336 °C mean  $\pm$  SD) than the eTeC treatment ( $30.4 \pm 2.3$  °C), however the difference  
337 between aTaC ( $29.0 \pm 2.2$  °C) and eTaC ( $30.3 \pm 2.4$  °C) was marginally insignificant  
338 ( $P = 0.07$ , Tukey post-hoc test, Figure 1a). Mean daily CO<sub>2</sub> concentration was  
339 significantly higher in the aTeC and eTeC treatments ( $829.9 \pm 71.6$  ppm and  $836.7 \pm$   
340  $70.6$  ppm, respectively, Figure 1b) than the ambient CO<sub>2</sub> treatments, however the  
341 concentration in the eTaC chamber ( $399.0 \pm 8.9$  ppm) was significantly lower than the  
342 aTaC chamber ( $459.2 \pm 12.2$  ppm). Relative humidity also varied by treatment with  
343 lower values in the elevated CO<sub>2</sub> treatments (Figure 2c), and  $D$  was higher in elevated  
344 temperature treatments, significantly so for eTeC (Figure 2d).

345

### 346 3.2 Stomatal Conductance

347

348 Analysing  $g_s$  data with measurements at all times of day pooled,  $g_s$  was significantly  
349 lower under the elevated temperature treatments ( $P = 0.0001$ , mixed effects model

350 with leaf as a random factor), with no significant effect of CO<sub>2</sub> treatment (Figure 3).

351 Conductance was highest in the control treatment and similarly low in both elevated

352 temperature treatments, with an intermediate  $g_s$  in the aTeC treatment (Figure 3).

353

354 The best mixed effects model of  $g_s$  accounting for microclimate and diurnal changes

355 included time of day, PAR,  $D_L$ , and interactions between  $D_L$ , warming treatment and

356 CO<sub>2</sub> treatment (Figure 4, Table 1). The overall pseudo marginal R<sup>2</sup> of the model was

357 0.38. If the random effect of leaf is also accounted for, the pseudo conditional R<sup>2</sup>

358 increases to 0.67 showing that there is high leaf-to-leaf variation in  $g_s$  (Supplementary

359 Figure 6). Interaction plots (Figure 4) of the model show that the relationship between

360  $g_s$  and  $D_L$  was weak (with no significant effect of  $D_L$  alone, Table 1) and varied

361 between treatments (interactions between heat treatment and  $D_L$ , and heat treatment,

362 CO<sub>2</sub> treatment and  $D_L$  were significant, Table 1). Under the aTeC and eTeC

363 treatments  $g_s$  was fairly invariant with  $D_L$ , whilst under the eTaC treatment  $g_s$

364 declined with  $D_L$  and under the control aTaC treatment  $g_s$  increased with  $D_L$ .

365 However, there is large scatter in the data (Figure 4, Figure S6).

366

367 The parameter  $g_l$  (inversely proportional with the carbon cost of transpiration and

368 hence low when a plant is conservative in its water use) estimated from the A-T<sub>L</sub>

369 curves did not show any significant differences between chambers, despite a lower

370 mean for the eTaC chamber (Figure 5).

371

372 *3.3 Observed Leaf Temperatures*

373

374 Diurnal patterns of average  $\Delta T_L$ ,  $T_L$ , PAR and  $D$  are shown for all chambers in Figure  
375 6 based on the period 24 February – 15 March 2017. There are differences in the  
376 patterns of average  $\Delta T_L$  for each chamber (Figure 6c,d), and these patterns are linked  
377 to the patterns of average PAR (Figure 6e,f). In order to properly compare the leaf  
378 temperatures between different leaves and chambers, the varying microclimate needs  
379 to be accounted for.

380

381 Mean  $\Delta T_L$  values were not significantly different between elevated and ambient CO<sub>2</sub>  
382 within the warming treatment under any specified microclimate (Figure 7, eTeC  
383 versus eTaC). In contrast, under the majority of microclimates tested  $\Delta T_L$  values were  
384 significantly higher in the elevated CO<sub>2</sub> treatment compared to the ambient CO<sub>2</sub>  
385 treatment when under ambient temperatures (Figure 7, aTeC versus aTaC). The  
386 microclimate conditions under which no significant differences were found were both  
387 in the high PAR category where there were much fewer data points, and the pattern in  
388 the data was similar to other microclimates. The extent of the difference in  $\Delta T_L$   
389 between aTaC and aTeC increased under increasing air temperature and increasing  
390 PAR, with a difference of 2.8 °C under high PAR and high air temperature. Analysing  
391 the data for  $T_L$  rather than  $\Delta T_L$  produced the same results (data not shown).

392

### 393 *3.4 Photosynthetic Temperature Response Curves*

394

395 Despite measuring photosynthesis at leaf temperatures up to 40 °C, there was no  
396 evidence of reaching  $T_{opt}$  as  $A$  continued to increase with  $T_L$  for the majority of leaves  
397 (Figure 8). Consequently, estimation of  $T_{opt}$  was not attempted and linear models were  
398 used to analyse the  $A$ - $T_L$  curves. There was no significant effect of temperature

399 treatment, however  $T_L$ , CO<sub>2</sub> treatment and their interaction were included in the best  
400 model.  $A$  (measured at the growth CO<sub>2</sub> concentration) was higher and the slope of the  
401  $A$ - $T$  relationship was steeper under the elevated CO<sub>2</sub> treatments (Figure 8). The  
402 marginal pseudo-R<sup>2</sup> of the model was 0.53, and all model terms ( $T_L$ , CO<sub>2</sub> treatment  
403 and their interaction) were significant (Table 2).

404

### 405 *3.5 Temperature Responses of $V_{cmax}$ and $J_{max}$*

406

407 As for  $A$ , both  $V_{cmax}$  and  $J_{max}$  increased with measurement temperature (Figure 9) and  
408 no optimum temperature was found within the measurement range (20 – 35 °C).

409  $V_{cmax}$  varied ranged 6.1 – 51.8  $\mu\text{mol m}^{-2} \text{s}^{-1}$  and  $J_{max}$  ranged 16.3 – 46.3  $\mu\text{mol m}^{-2} \text{s}^{-1}$   
410 with standard errors ranging 0.097 – 6.88  $\mu\text{mol m}^{-2} \text{s}^{-1}$  for  $V_{cmax}$  and 0.29 - 2.76  $\mu\text{mol}$   
411  $\text{m}^{-2} \text{s}^{-1}$  for  $J_{max}$ . The higher SE values correspond with higher parameter values.

412 Temperature treatment had no significant effect on either of the two variables,  
413 however  $V_{cmax}$  was lower and the temperature response of  $V_{cmax}$  was weaker (lower  
414 activation energy) under elevated CO<sub>2</sub>, with significant differences between eTaC and  
415 eTeC treatments (Figure 9, Table 3). The ratio of  $J_{max}/V_{cmax}$  decreased with increasing  
416 temperature (30 - 35 °C, not sufficient  $J_{max}$  data at 20°C), and was significantly higher  
417 in the elevated CO<sub>2</sub> treatment (Figure S7).

418

### 419 *3.6 Seedling growth*

420

421 There were no significant effects of treatment on seedling size at any time point  
422 during the experiment (vertical height, total branch length, number of leaves, Figure  
423 S8).

424

## 425 4. Discussion

426

427 In this study we present a factorial elevated temperature and elevated CO<sub>2</sub> experiment  
428 with juveniles of a tropical pioneer species. The study was performed under high  
429 temperature conditions including a heatwave during the acclimation period (Figure 1).

430 Our key findings are i) that the elevated temperature treatment had a stronger  
431 influence on  $g_s$  than elevated CO<sub>2</sub> (Figure 3, Table 1), ii) that reduced  $g_s$  caused a  
432 change in leaf temperatures (Figure 7), iii) that net photosynthesis and photosynthetic  
433 capacities show very high temperature tolerances with no evidence for acclimation to  
434 the elevated temperature treatment (Figure 8), and iv) that there was no interactive  
435 effect of temperature and CO<sub>2</sub> treatment on  $g_s$  (Figure 3, Table 1)

436

### 437 *4.1 Temperature and CO<sub>2</sub> impacts on stomatal conductance*

438

439 As expected,  $g_s$  declined in the eC treatments compared with the control, as has been  
440 shown in many other studies. Here we find a 21.2 % reduction (95% CI 10.6 – 30.2 %  
441 based on bootstrapping) in our aTeC treatment compared with the control (Figure 2).

442 In forest free air CO<sub>2</sub> enrichment (FACE) experiments with CO<sub>2</sub> elevated by 200 ppm  
443  $g_s$  declines on average by *c.* 20 % (Ainsworth & Rogers 2007), with stronger declines  
444 in angiosperm than gymnosperm species (Brodribb et al. 2009). Past chamber  
445 experiments performed on angiosperm trees with a doubling of CO<sub>2</sub> show an average  
446  $g_s$  reduction of *c.* 18 % (from data in Saxe et al. 1998). Our data therefore shows  
447 consistency with species from other biomes, but with few tropical species included in  
448 existing studies. The literature on tropical species shows wide variation (Berryman et

449 al. 1994, Goodfellow et al. 1997, Liang et al. 2001, Leakey et al. 2002, Khurana &  
450 Singh 2004, Cernusak et al. 2011, Dalling et al. 2016, Wahidah et al. 2017). Data  
451 from eight publications covering 22 tropical angiosperm species with CO<sub>2</sub> enrichment  
452 in the range 300-400 ppm showed an average change in  $g_s$  of  $28.6 \pm 18.4$  % SD  
453 reduction. One species (*Chrysophyllum cainito*) showed a very small increase  
454 (Dalling et al. 2016), and the largest reduction of 61 % was shown by *Inga punctata*  
455 (Cernusak et al. 2011). Hence, the reduction we observed was below average but well  
456 within the range of observations of other tropical species in experiments.

457

458 A limitation of our experiment and its comparability with other studies is the short  
459 duration of exposure to the treatments. We measured the physiological responses on  
460 leaves formed before initiation of the experiment, which had been exposed to the  
461 treatments for *c.* 5 weeks. As stomatal properties (e.g. density) often differ on leaves  
462 formed in high CO<sub>2</sub> environments (Saxe et al. 1998), there could potentially be  
463 greater changes than we observed, had new leaves formed. Whilst this is quite  
464 possible, the long-term response of  $g_s$  to CO<sub>2</sub> is typically similar to the short term  
465 response (Way et al. 2015), and hence while the mechanism of reduced  $g_s$  may be  
466 different in short and long-term studies, the  $g_s$  may be similar. However, a caveat to  
467 our results is that to truly observe the acclimation of leaves to the treatments, longer  
468 acclimation periods and production of new leaves is necessary.

469

470 The observed responses of  $g_s$  to elevated temperature vary considerably in the few  
471 studies available (Way et al. 2015). Here we find strong reductions in  $g_s$  in the  
472 temperature treatments with a 49.6 % (95% CI 42.2 – 56.5 %) reduction under the  
473 eTaC treatment and 53.0 % (95% CI 52.9 – 58.3 %) reduction in the combined eTeC

474 treatment, although we did not find any significant difference between treatments for  
475 the  $g_l$  parameter value. This may be because the Medlyn et al. (2011) model  
476 incorporates the ambient CO<sub>2</sub> concentration, and if the short-term and long term  $g_s$   
477 response to CO<sub>2</sub> is the same there would not be a difference. The declines in  $g_s$  are not  
478 driven purely by higher  $D_L$  in the eT chambers as there are significant differences  
479 even when  $D_L$  is controlled for (Table 1, Figure 4) or when  $g_s$  is analysed within a  
480 narrow  $D_L$  range (data not shown). This shows acclimation of  $g_s$  due to higher air  
481 temperature and/or  $D_L$  (both quantities strongly co-varied) which will reduce water  
482 loss from the plants. There were no significant differences in  $g_s$  between the eTaC and  
483 eTeC treatments, hence the response to the temperature treatment (with significant  
484 differences) was stronger than the response to the CO<sub>2</sub> treatment. The result is  
485 surprising given the very mixed results in the limited literature on elevated  
486 temperature impacts on  $g_s$ , and even more so given that in this study the temperature  
487 treatment was fairly modest (+1.5 °C) compared to the CO<sub>2</sub> treatment (+ 400 ppm),  
488 although the effect of eC on  $g_s$  may have been limited by the lack of new leaf  
489 development (as stated above). This finding could also be because the ambient  
490 temperatures were very hot inside the chambers throughout the experiment and  
491 especially during the acclimation phase (Figure 1), which meant that a small increase  
492 in air temperature had a large impact, with stomata closing to reduce water loss. An  
493 experimental study of gas exchange of *Solanum lycopersicum* (cherry tomato)  
494 measured during and following a +14 °C heatwave showed reduced  $g_s$  during the  
495 heatwave, which remained low when measured 5 days after the heatwave (Duan et al.,  
496 2016). Similarly, Duarte et al. (2016) found reduced  $g_s$  of *Pseudotsuga menziesii*  
497 (Douglas fir) during +12 °C heatwaves which remained when measured one month  
498 later. This is somewhat in contrast with recent research suggesting stomata remain

499 open under very high air temperatures for increased evaporative cooling (Slot et al.,  
500 2016, Slot & Winter 2017b, Urban et al., 2017, Drake et al, 2018). Responses are  
501 likely to be species specific, with an example of a late successional species reducing  
502  $g_s$  under heatwave conditions while a pioneer species showed increased  $g_s$  (Vargas &  
503 Cordero 2013). However these studies are assessing the instantaneous response of  $g_s$   
504 to short-term warming rather than the long-term response. A field study reporting the  
505 impact of four months of experimentally elevated temperature on  $g_s$  of existing leaves  
506 showed a *c.* 25 % reduction with 2 °C temperature increase averaged across six  
507 tropical species (Doughty 2011), lower than we observed. However, in contrast to our  
508 results for *Alchornea glandulosa*, Yepes Mayorga (2010) found that  $g_s$  of *Hymenea*  
509 *courbaril* was more strongly controlled by elevated CO<sub>2</sub> than elevated temperature in  
510 a similar study, as did Ameye et al. (2012) in a study of temperate species *Quercus*  
511 *rubra* and *Pinus taeda* in treatments of elevated by 320 ppm and T<sub>A</sub> elevated by 3 °C  
512 or with heat waves. Two studies of subtropical/temperate *Eucalyptus* spp. found no  
513 difference in  $g_s$  of under treatments of CO<sub>2</sub> elevated by 240 ppm and T<sub>A</sub> elevated by 3  
514 °C or 4 °C after 15 and 7 months of acclimation respectively (Quentin et al. 2013,  
515 Duan et al. 2018). While more studies are needed to see if there is a general pattern  
516 for tropical broadleaf species, the results of this study suggest that there could be  
517 larger implications of rising temperature than rising CO<sub>2</sub> for water use of at least  
518 some species of tropical tree, and even implications of modest temperature rises such  
519 as the ambitious aims of the Paris Agreement (UNFCCC 2015).

520

521 The  $g_s$  dataset also showed a weak relationship with respect to  $D_L$ , which varied with  
522 treatment (Table 1, Figure 3). Other studies with a congeneric species show that  $g_s$  of  
523 *A. triplinervia* is more weakly linked to  $D_L$  than other measured species (García-

524 Núñez et al. 1995, Fauset et al. 2018). A weaker relationship between  $g_s$  and  $D_L$  is  
525 expected for low wood density pioneer species compared to species with higher wood  
526 density (Lin et al. 2015). In addition, as the species is commonly found in riparian  
527 areas (and therefore with access to a good water supply), its lack of stomatal control is  
528 not surprising. Our results show that despite a weak instantaneous response of  $g_s$  to  
529 microclimate, *A. glandulosa* still showed acclimation and reduction in  $g_s$  in response  
530 to long-term microclimate change. Hence, the short-term response of  $g_s$  does not  
531 provide information on the long-term response.

532

#### 533 4.2 $CO_2$ impacts on leaf temperature

534

535 The lower  $g_s$  as a result of elevated  $CO_2$  caused increases in leaf temperatures (Figure  
536 5). The differences in  $\Delta T_L$  increased with increasing PAR at the leaf surface, and to a  
537 lesser extent with increasing air temperature and  $D$ . This shows that the differences in  
538 leaf temperatures due to  $CO_2$ -altered  $g_s$  are more apparent under high thermal stress  
539 conditions (high PAR and high air temperature), and therefore that this impact is  
540 likely to be stronger under heat waves, which are expected to increase in frequency  
541 during the 21<sup>st</sup> century (Coumou & Robinson 2013). When at high air temperatures,  
542 differences in  $\Delta T_L$  due to reduced  $g_s$  could have significant consequences, as seen in  
543 observations of premature leaf senescence during a heatwave in a temperate FACE  
544 experiment (Warren et al. 2011). While the average differences in  $\Delta T_L$  between aTaC  
545 and aTeC reached 2.8 °C under high light and air temperature, the light conditions  
546 were limited by the greenhouse environment which reached only 1000  $\mu\text{mol m}^{-2} \text{s}^{-1}$ .  
547 Under field conditions where incoming PAR can reach over 2500  $\mu\text{mol m}^{-2} \text{s}^{-1}$  the  
548 impact of reduced  $g_s$  on  $\Delta T_L$  could be much higher. Unfortunately due to  $\Delta T_L$

549 fluctuations induced by heating the air (Figure S3) it was not possible to assess the  
550 impact of the high temperature treatment compared to the control. Within the two  
551 high temperature treatments there were no significant differences in  $\Delta T_L$  under any  
552 microclimate between the elevated and ambient CO<sub>2</sub> treatments, which is expected as  
553 they did not show any significant differences in  $g_s$ .

554

#### 555 4.3 Temperature and CO<sub>2</sub> impacts on photosynthesis

556

557 The elevated temperature treatment had no discernible effect on  $A$  or photosynthetic  
558 capacity and their responses to elevated temperatures. The high temperature tolerance  
559 of both  $A$  and photosynthetic capacity was marked, with no decline in  $A$  found even at  
560 40 °C. Consequently, we were not able to assess shifts in  $T_{opt}$  with treatment as  $T_{opt}$   
561 was above the maximum temperature under which we performed measurements. It is  
562 worth noting that such high leaf temperatures are often considered to be detrimental to  
563 photosynthetic functions (e.g. Rubisco activase activity is strongly temperature  
564 sensitive with inhibition found above 35 °C [Crafts-Brandner & Salvucci 2000]).  
565 Moreover, photosystem II (PSII) activity declines rapidly above temperature  
566 thresholds of 41.5 – 50.8 °C (O’Sullivan et al. 2017). However, plants are well  
567 adapted to their environment, with temperature thresholds of PSII increasing from  
568 arctic to tropical habitats (O’Sullivan et al. 2017), and even increasing thermal  
569 tolerance of PSII over very short timescales (days) in response to high temperatures  
570 (Drake et al. 2018). Slot et al. (2017c) found that  $T_{opt}$  measured in the field in Panama  
571 was around the mean maximum daily temperature (30-32 °C) for all 42 species  
572 measured, and that, for a smaller sample of four species, it was  $g_s$  rather than Rubisco  
573 activase,  $J_{max}$ ,  $V_{cmax}$  or light respiration that limited the photosynthetic rates at high

574 temperatures (Slot & Winter 2017a). In another study,  $T_{opt}$  was higher than daily  
575 maximum air temperature in moist and wet tropical forest sites in Puerto Rico (Mau et  
576 al. 2018). In the case of the *A. glandulosa* seedlings measured here, the mean  
577 maximum daily temperature over the acclimation and measurement period was 40 –  
578 42 °C (varying by treatment, Figure 1), matching the minimum potential  $T_{opt}$  of 40 °C,  
579 and showing tolerance to the high temperatures to which they were exposed.  
580 Measurement under higher temperatures would be necessary to find the  $T_{opt}$  for these  
581 plants. Over the measured temperature range,  $g_s$ ,  $V_{cmax}$  and  $J_{max}$  did not decline. Yet, it  
582 should also be noted that the rates of  $A$ ,  $V_{cmax}$  and  $J_{max}$  were fairly low (c. 3, 40 and 35  
583  $\mu\text{mol m}^{-2} \text{s}^{-1}$  respectively, at the highest values and under ambient  $\text{CO}_2$ ). For example,  
584 these are lower than  $A$  of 12 – 16  $\mu\text{mol m}^{-2} \text{s}^{-1}$  across 42 Panamanian species (Slot &  
585 Winter 2017c) and 5 – 12  $\mu\text{mol m}^{-2} \text{s}^{-1}$  for four species in Puerto Rico (Mau et al.  
586 2018), and  $V_{cmax}$  of 70 – 300  $\mu\text{mol m}^{-2} \text{s}^{-1}$  and  $J_{max}$  of 80 – 220  $\mu\text{mol m}^{-2} \text{s}^{-1}$  across four  
587 Panamanian species (Slot & Winter 2017a), all at their optimum temperatures. The  
588 measured rates are also lower than plants in other high temperature environments e.g.  
589 five desert species with  $A$  ranging 19 – 35  $\mu\text{mol m}^{-2} \text{s}^{-1}$  (Mooney et al. 1981), and  
590 Mediterranean cork oak with  $V_{cmax}$  and  $J_{max}$  both over 150  $\mu\text{mol m}^{-2} \text{s}^{-1}$  (Ghouil et al.  
591 2003). Thus, high temperature tolerance of photosynthetic machinery in *A. glandulosa*  
592 may come at a cost of lower photosynthetic rates. An alternative explanation for the  
593 low photosynthetic rates is the low light conditions within the greenhouse, with  
594 maximum leaf surface PAR of 800-1000  $\mu\text{mol m}^{-2} \text{s}^{-1}$ . In the field, maximum PAR is  
595 likely to be much higher ( $> 2000 \mu\text{mol m}^{-2} \text{s}^{-1}$ ), and leaves may achieve higher  
596 photosynthetic rates. The low light conditions in the greenhouse also have  
597 implications for the high temperature tolerance observed. Because at high  
598 temperatures photosynthetic biochemistry is under greater stress, there is a greater

599 need for photoprotection from high incoming radiation. Perhaps under the higher light  
600 conditions found in the field, very high temperature tolerance of photosynthesis may  
601 be more difficult to achieve. Field studies under high temperature conditions are  
602 needed to establish whether the high tolerance we find here also occurs under natural  
603 conditions.

604

605 As for  $g_s$ , the impacts of increased CO<sub>2</sub> followed expectations from previous studies  
606 with increased net photosynthesis when measured at growth CO<sub>2</sub>, a steeper slope of  $A$   
607 in response to temperature, and downregulation of photosynthetic capacity (Figure 8,  
608 9). The steeper slope is due to the reduction in oxygenation of Rubisco due to higher  
609  $c_i$  under elevated CO<sub>2</sub>, which otherwise increases with temperature due to the reduced  
610 affinity of Rubisco for CO<sub>2</sub> with higher temperature (Long 1991). The effect of the  
611 downregulation can be seen when the temperature response of  $A$  is plotted with added  
612 points taken from the  $A$ - $c_i$  curves at 400 and 800 ppm CO<sub>2</sub> for the elevated and  
613 ambient CO<sub>2</sub> treatments respectively, showing that without the downregulation of  
614 photosynthetic capacity  $A$  would have been higher in the elevated CO<sub>2</sub> treatment  
615 (Figure S9).

616

#### 617 *4.4 Conclusions*

618

619 This study demonstrates that the tropical tree species *Alchornea glandulosa* shows  
620 strong responses of stomatal conductance to elevated temperature and of  
621 photosynthetic parameters to elevated CO<sub>2</sub>. While a very high temperature tolerance  
622 of photosynthesis was observed in this species, photosynthetic rates were low under  
623 the high growth temperatures. These results show that this species will be able to cope

624 with the predicted atmospheric changes over the coming century. Therefore, it is an  
625 appropriate species for reforestation activities, which are planned and ongoing in the  
626 Atlantic forest (Rodrigues et al. 2009). More studies of other species are required to  
627 determine whether similar results occur in other forest trees.

628

## 629 5. Acknowledgements

630 We thank Viviane Costa at the Lafieco greenhouse, and Santiago Clerici and David  
631 Ashley at the University of Leeds, for considerable assistance with this project. We  
632 acknowledge funding from Natural Environment Research Council/NERC  
633 (NE/K01644X/1 and NE/N012542/1) and the State of São Paulo Research  
634 Foundation/FAPESP (2012/51509-8, 2012/51872-5) as part of the projects ECOFOR  
635 and BIODRED and the European Research Council project GEM-TRAIT awarded to  
636 Yadvinder Malhi.

637

## 638 6. CRediT Author Statement

639 Sophie Fauset: Conceptualization, Formal Analysis, Investigation, Writing – Original  
640 Draft, Lauana Oliveira: Investigation, Writing – Review & Editing, Marcos  
641 Buckeridge: Resources, Conceptualization, Writing – Review & Editing, Christine H.  
642 Foyer: Writing – Review & Editing, David Galbraith: Funding Acquisition, Writing –  
643 Review & Editing, Rakesh Tiwari: Writing – Review & Editing, Manuel Gloor:  
644 Conceptualization, Funding Acquisition, Writing – Review & Editing.

645

## 646 7. References

647

648 Aidar, M.P.M., Martinez, C.A., Costa A.C., Costa, P.M.F., Dietrich, S.M.C.,  
649 Buckeridge, M.S., 2002. Effect of atmospheric CO<sub>2</sub> enrichment on the establishment  
650 of seedlings of jatobá, *Hymenaea courbaril* L. (Leguminosae, Caesalpinioideae).  
651 Biota Neotropica 2 (1).  
652  
653 Ainsworth, E.A., Rogers, A., 2007. The response of photosynthesis and stomatal  
654 conductance to rising [CO<sub>2</sub>]: mechanisms and environmental interactions. Plant Cell  
655 Env. 30, 258-270.  
656  
657 Ameye, T., Wertin, T.W., Bauweraerts, I., McGuire, M.A., Teskey, R.O., Steppe, K.,  
658 2012. The effect of induced heat waves on *Pinus taeda* and *Quercus rubra* seedlings  
659 in ambient and elevated CO<sub>2</sub> atmospheres. New Phytol. 196, 448-461.  
660  
661 Bartoń, K., 2016. MuMIn: Multi-Model Inference. R Package version 1.15.16.  
662  
663 Becklin, K.M., Walker II., S.M., Way, D.A., Ward, J.K., 2017. CO<sub>2</sub> studies remain  
664 key to understanding a future world. New Phytol. 214, 34-40.  
665  
666 Berryman, C.A., Eamus, D., Duff, G.A., 1994. Stomatal responses to a range of  
667 variables in two tropical tree species grown with CO<sub>2</sub> enrichment. J. Exp. Bot. 45,  
668 539-546.  
669  
670 Brodribb, T., McAdam, S.A.M., Jordan, G.J., Feild, T.S., 2009. Evolution of stomatal  
671 responsiveness to CO<sub>2</sub> and optimization of water-use efficiency among land plants.  
672 New Phytol. 183, 839-847.

673

674 Collins, M., Knutti, R., Arblaster, J., Dufresne, J.-L., Fichefet, T., Friedlingstein, P.,  
675 ..., Wehner, M., 2013. Long-term climate change: Projections, commitments and  
676 irreversibility. In: *Climate Change 2013: The Physical Science Basis. Contribution of*  
677 *working group I to the Fifth Assessment Report of the Intergovernmental Panel on*  
678 *Climate Change* (eds Stocker, T.F., Qin, D., Plattner, G.-K., Tignor, M., Allen, S.K.,  
679 Boschung, J., ..., Midgley, P.M.), pp 1029-1136, Cambridge University Press,  
680 Cambridge, UK and New York, USA.

681

682 Cernusak, L.A., Winter, K., Martínez, C., Correa, E., Aranda, J., Garcia, M.,  
683 Jaramillo, C., Turner, B.L., 2011. Responses of legume versus nonlegume tropical  
684 tree seedlings to elevated CO<sub>2</sub> concentration. *Plant Physiol.* 157, 372-385.

685

686 Coumou, D., Robinson, A., 2013. Historic and future increase in the global land area  
687 affected by monthly heat extremes. *Environ. Res. Lett.* 8, 034018.

688

689 Crafts-Brandner, S.J., Salvucci, M.E., 2000. Rubisco activase constrains the  
690 photosynthetic potential of leaves at high temperature and CO<sub>2</sub>. *Proc. Nat. Acad. Sci.*  
691 2000, 13430-13435.

692

693 Dalling, J.W., Cernusak, L.A., Winter, K., Aranda, J., Garcia, M., Virgo, A.,  
694 Cheesman, A.W., Baresch, A., Jaramillo, C., Turner, B.L., 2016. Two tropical  
695 conifers show strong growth and water-use efficiency responses to altered CO<sub>2</sub>  
696 concentration. *Annals Bot.* 118, 1113-1125.

697

698 De Souza, A.P., Gaspar, M., da Silva E.A., Ulian, E.C., Waclawovsky, A.J.,  
699 Nishiyama Jr., M.Y., ..., Buckeridge, M.S., 2008. Elevated CO<sub>2</sub> increases  
700 photosynthesis, biomass and productivity, and modifies gene expression in sugarcane.  
701 *Plant Cell Environ.* 31, 1116–1127  
702  
703 Doughty, C.E., Goulden, M.L., 2008. Are tropical forests near a high temperature  
704 threshold? *J. Geophys. Res.* 113, G00B07.  
705  
706 Doughty, C.E., 2011. An in situ leaf and branch warming experiment in the Amazon.  
707 *Biotropica* 43, 658-665.  
708  
709 Drake, B.G., González-Meler, M.A., Long, S.P., 1997. More efficient plants: A  
710 consequence of rising atmospheric CO<sub>2</sub>? *Annu. Rev. Plant Phys.* 48, 609-639.  
711  
712 Drake, J.E., Tjoelker, M.G., Vårhammar, A., Medlyn, B.E., Reich, P.B., Leigh, A.,  
713 ..., Barton, C.V.M., 2018. Trees tolerate an extreme heatwave via sustained  
714 transpirational cooling and increased leaf thermal tolerance. *Glob. Change Biol.*  
715 10.1111/gcb.14037.  
716  
717 Duan, H., Chaszar, B., Lewis, J.D., Smith, R.A., Huxman, T.E., Tissue, D.T., 2018.  
718 CO<sub>2</sub> and temperature effects on morphological and physiological traits of drought-  
719 induces mortality. *Tree Physiology* 38, 1138-1151.  
720  
721 Duarte, A.G., Katata, G., Hoshika, Y., Hossain, M., Kreuzwieser, J., Arneth, A.,  
722 Ruehr, N.K. 2016. Immediate and potential long-term effects of consecutive heat

723 waves on the photosynthetic performance and water balance in Douglas-fir. *J. Plant*  
724 *Physiology* 205, 57-66.

725

726 Dusenage, M.E., Way, D.A., 2017. Warming puts the squeeze on photosynthesis –  
727 lessons from tropical trees. *J. Exp. Bot.* 68, 2073-2077.

728

729 Duursma, R.A. 2015. Plantecophys – an R package for analysing and modelling leaf  
730 gas exchange data. *PLoS ONE* 10, e0143346.

731

732 Fauset, S., Gloor, E.U., Aidar, M.P.M., Freitas, H.C., Fyllas, N.M., Marabesi, M.A.,  
733 ..., Joly, C.A., 2017. Tropical forest light regimes in a human-modified landscape.  
734 *Ecosphere* 8, e02002.

735

736 Fauset, S., Freitas, H.C., Galbraith, D.R., Sullivan, M.J.P., Aidar, P.M., Joly, C.A.,  
737 ..., Gloor, M.U., 2018. Differences in leaf thermoregulation and water use strategies  
738 between three co-occurring Atlantic forest tree species. *Plant Cell Env.* DOI:  
739 10.1111/pce.13208

740

741 Fielder, P., Comeau, P., 2000. Construction and testing of an inexpensive PAR  
742 sensor. Ministry of Forests Research Program. Victoria, British Columbia, Working  
743 Paper 53/2000.

744

745 García-Núñez C., Azócar, Rada, F., 1995. Photosynthetic acclimation to light in  
746 juveniles of two cloud forest tree species. *Trees* 10, 114-124.

747

748 Gaastra P., 1959. Photosynthesis of crop plants as influenced by light, carbon  
749 dioxide, temperature, and stomatal diffusion resistance. Mededel  
750 Landbouwho Gesch Wageningen 59, 1–68.  
751

752 GBIF Secretariat, 2017. *Alchornea glandulosa* Poepp. GBIF Backbone Taxonomy.  
753 Checklist Dataset <https://doi.org/10.15468/39omei> (accessed via GBIF.org 9 February  
754 2018).  
755

756 Ghannoum, O., Phillips, N.G., Sears, M.A., Logan, B.A., Lewis, J.D., Conroy, J.P.,  
757 Tissue, D.T., 2010. Photosynthetic responses of two eucalypts to industrial-age  
758 changes in atmospheric [CO<sub>2</sub>] and temperature. *Plant Cell Env* 33, 1671-1681.  
759

760 Ghouil, H., Montpied, P., Epron, D., Ksontini, M., Hanchi, B., Dreyer, E., 2003.  
761 Thermal optima of photosynthetic functions and thermostability of photochemistry in  
762 cork oak seedlings. *Tree Physiology* 23, 1031-1039.  
763

764 Goodfellow, J., Eamus, D., Duff, G., 1997. Diurnal and seasonal changes in the  
765 impact of CO<sub>2</sub> enrichment on assimilation, stomatal conductance and growth in a  
766 longterm study of *Manigifera indica* in the wet-dry tropics of Australia. *Tree*  
767 *Physiology* 17, 291-299.  
768

769 Janzen, D.H., 1967. Why mountain passes are higher in the tropics. *Am. Nat.* 101,  
770 233-249.  
771

772 Jones H.G., 1992. Plants and microclimate. Cambridge University Press, Cambridge,  
773 UK.  
774

775 Khurana E., Singh, J.S., 2004, Response of five dry tropical tree species to elevated  
776 CO<sub>2</sub>: impact of seed size and successional status. *New Forests*, 27, 139-157.  
777

778 Körner, C., Würth, M., 1996. A simple method for testing leaf responses of tall  
779 tropical forest trees to elevated CO<sub>2</sub>. *Oecologia* 107, 421-425.  
780

781 Leakey, A.D.B., Bishop, K.A., Ainsworth, E.A., 2012. A multi-biome gap in  
782 understanding of crop and ecosystem responses to elevated CO<sub>2</sub>. *Curr. Opin. Plant*  
783 *Biol.* 15, 228-236.  
784

785 Leakey, A.D.B., Press, M.C., Scholes, J.D., Watling, J.R., 2002. Relative  
786 enhancement of photosynthesis and growth at elevated CO<sub>2</sub> is greater under sunflecks  
787 than uniform irradiance in a tropical rain forest tree seedling. *Plant Cell Environ.* 25,  
788 1701-1714.  
789

790 Lewis, J.D., Lucash, M., Olszyk, D.M., Tingley, D.T., 2002. Stomatal responses of  
791 Douglas-fir seedlings to elevated carbon dioxide and temperature during the third and  
792 fourth years of exposure. *Plant Cell Env.* 25, 1411-1421.  
793

794 Liang, N., Tang, Y., Okuda, T., 2001. Is elevation of carbon dioxide concentration  
795 beneficial to seedling photosynthesis in the understorey of tropical rain forests? *Tree*  
796 *Physiology* 21, 1047-1055.

797 Lin, Y.-S., Medlyn, B.E., Duursma, R.A., Prentice, I.C., Wang, H., Baig, S., ...,  
798 Wingate, L., 2015. Optimal stomatal behaviour around the world. *Nat. Clim. Change*  
799 5, 459-464.  
800

801 Liu, Y.Y., van Dijk, A.I.J.M., de Jeu, R.A.M., Canadell, J.G., McCabe, M.F., Evans,  
802 J.P., Wang, G., 2015. Recent reversal in loss of global terrestrial biomass. *Nat. Clim.*  
803 *Change* 5, 470-474.  
804

805 Long, S.P., 1991. Modification of the response of photosynthetic productivity to  
806 rising temperature by atmospheric CO<sub>2</sub> concentrations: Has its importance been  
807 underestimated? *Plant Cell Env.* 14, 729-739.  
808

809 Lovelock, C.E., Virgo, A., Popp, M., Winter, K., 1999. Effects of elevated CO<sub>2</sub>  
810 concentration on photosynthesis, growth and reproduction of branches of the tropical  
811 canopy tree species, *Luehea seemannii* Tr. & Planch. *Plant Cell Env.* 22, 49-59.  
812

813 Mau, A.C., Reed, S.C., Wood, T.E., Cavaleri, M.A., 2018. Temperate and tropical  
814 forest canopies are already functioning beyond their thermal thresholds for  
815 photosynthesis. *Forests* 9, doi:10.3390/f9010047.  
816

817 Medlyn, B.E., Dreyer, E., Ellsworth, D., Forstreuter, M., Harley, P.C., Kirshbaum,  
818 M.U.F., ..., Loustau, D., 2002. Temperature response of parameters of a  
819 biochemically based model of photosynthesis. II. A review of experimental data.  
820 *Plant Cell Env.* 25, 1167-1179.  
821

822 Medlyn, B.E., Duursma, R.A., Eamus, D., Ellsworth, D.S., Prentice, I.C., Barton,  
823 C.V.M., ..., Wingate, L., 2011. Reconciling the optimal and empirical approaches to  
824 modelling stomatal conductance. *Global Change Biol.* 17, 2134-2144.  
825

826 Mooney, H.A., Field, C., Gulmon, S.L., Bazzaz, F.A., 1981. Photosynthetic capacity  
827 in relation to leaf position in desert versus old-field annuals. *Oecologia*, 50, 109-112.  
828

829 Nakagawa, S., Schielzeth., H. 2013. A general and simple method for obtaining R<sup>2</sup>  
830 from generalized linear mixed-effects models. *Methods Ecol. Evol.* 4, 133–142.  
831

832 Oren, R., Sperry, J.S., Katul, G.G., Pataki, D.E., Ewers, B.E., Phillips, N., Schäfer,  
833 K.V.R., 1999. Survey and synthesis of intra- and interspecific variation in stomatal  
834 sensitivity to vapour pressure deficit. *Plant Cell Env.* 22, 1515-1526.  
835

836 O’Sullivan, O.S., Heskell, M.A., Reich, P.B., Tjoelker, M.G., Weerasinghe, L.K.,  
837 Penillard, A., ..., Atkin, O.K. 2017. Thermal limits of leaf metabolism across biomes.  
838 *Glob. Change Biol.* 23, 209-223.  
839

840 Pan, Y., Birdsey, R.A., Fang, J., Houghton, R., Kauppi, P.E., Kurz W.A., ..., Hayes  
841 D. 2011., A large and persistent carbon sink in the world’s forests. *Science* 333, 988-  
842 993.  
843

844 Pascotto, M.C., 2006. Avifauna dispersora de sementes de *Alchornea glandulosa*  
845 (Euphorbiaceae) em uma área de mata ciliar no estado de São Paulo. *Revista*  
846 *Brasileira de Ornithologia* 14, 291-296.

847

848 Pinheiro, J., Bates, D., DebRoy, S., Sarkar, D., Core Team, R. 2017. nlme: Linear and  
849 nonlinear mixed effects models. R Package Version, 3.1–131.

850

851 Quentin, A.G., Crous, K.Y., Barton, C.V.M., Ellsworth, D.S, 2013. Photosynthetic  
852 enhancement by elevated CO<sub>2</sub> depends on seasonal temperatures for warmed and non-  
853 warmed *Eucalyptus globulus* trees. *Tree Physiology* 35, 1249-1263.

854

855 Robakowski, P., Li, Y., Reich, P.B. 2012. Local ecotypic and species range-related  
856 adaptation influence photosynthetic temperature optima in deciduous broadleaved  
857 trees. *Plant Ecol.* 213, 113-125.

858

859 Rodrigues, R.R., Lima, R.A.F., Gandolfi, S., Nave, A.G., 2009. On the restoration of  
860 high diversity forests: 30 years of experience in the Brazilian Atlantic Forest. *Biol.*  
861 *Conserv.* 142, 1242-1251.

862

863 Russo, S., Sillmann, J., Fischer, E.M., 2015. Top ten European heatwaves since 1950  
864 and their occurrence in the coming decades. *Env. Res. Lett.* 10, 124003.

865

866 Saxe, H., Ellsworth, D.S., Heath, J., 1998. Tree and forest functioning in an enriched  
867 CO<sub>2</sub> atmosphere. *New Phytol.*, 139, 395-436.

868

869 Siebke, K., Ghannoum, O., Conroy, J.P., von Caemmerer, S., 2002. Elevated CO<sub>2</sub>  
870 increases the leaf temperature of two glasshouse-grown C<sub>4</sub> grasses. *Funct. Plant Biol.*  
871 29, 1377-1385.

872

873 Šigut, L., Holišová, P., Klem, K., Šprtová M., Calfapietra, C., Marek, M.V., Špunda,  
874 V., 2015. Does long-term cultivation of sapling under elevated CO<sub>2</sub> concentration  
875 influence their photosynthetic response to temperature? *Ann. Bot.* 166, 929-939.

876

877 Slot, M., Garcia, M.N., Winter, K., 2016. Temperature response of CO<sub>2</sub> exchange in  
878 three tropical tree species. *Funct. Plant Biol.* 43, 468-478.

879

880 Slot, M., Winter, K., 2017a. In situ temperature relationships of biochemical and  
881 stomatal controls of photosynthesis in four lowland tropical tree species. *Plant Cell*  
882 *Env.* 40, 3055-3068.

883

884 Slot, M., Winter, K., 2017b. Photosynthetic acclimation to warming in tropical forest  
885 tree seedlings. *J. Exp. Bot.* 68, 2275-2284.

886

887 Slot, M., Winter, K., 2017c. In situ temperature response of photosynthesis of 42 tree  
888 and liana species in the canopy of two Panamanian lowland tropical forests with  
889 contrasting rainfall regimes. *New Phytol.* 214, 1103-1117.

890

891 UNFCCC (2015) Adoption of the Paris Agreement, 21<sup>st</sup> Conference of Parties, Paris,  
892 United Nations.

893

894 Urban, J., Ingwers, M.W., McGuire, M.A., Teskey, R.O., 2017. Increase in leaf  
895 temperature opens stomata and decouples net photosynthesis from stomatal

896 conductance in *Pinus taeda* and *Populus deltoides x nigra*. *J. Exp. Bot.* 68, 1757-  
897 1767.

898

899 Vargas, G.G., Cordero R.A.S. 2013. Photosynthetic responses to temperature of two  
900 tropical rainforest tree species from Costa Rica. *Trees*, 27, 1261-1270.

901

902 Vårhammar, A., Wallin, G., McLean, C.M., Dusenge, M.E., Medlyn, B.E., Hasper,  
903 T.B., Nsabimana, D., Uddling, J., 2015. *New Phytol.* 206, 1000-1012.

904

905 Wahidah, M.N.L., Juliana, W.A.W., Nizam, M.S., Radziah, C.M.Z.C., 2017. Effects  
906 of elevated atmospheric CO<sub>2</sub> on photosynthesis, growth and biomass in *Shorea*  
907 *platycarpa* F. Heim (Meranti Paya). *Sains Malaysiana* 46, 1421-1428.

908

909 Warren, J.M., Norby, R.J., Wullschleger, S.D., 2011. Elevated CO<sub>2</sub> enhances leaf  
910 senescence during extreme drought in a temperate forest. *Tree Physiol.* 31, 117-130.

911

912 Way, D.A., Oren, R., Kroner, Y., 2015. The space-time continuum: the effects of  
913 elevated CO<sub>2</sub> and temperature and the importance of scaling. *Plant Cell Env.* 38, 991-  
914 1007.

915

916 Wertin, T.M., McGuire, M.A., Teskey, R.O., 2010. The influence of elevated  
917 temperature, elevated atmospheric CO<sub>2</sub> concentration and water stress on net  
918 photosynthesis of loblolly pine (*Pinus taeda* L.) at northern, central and southern sites  
919 in its native range. *Glob. Change Biol.* 16, 2089-2103.

920

921 Yamori, W., Hikosaka, K., Way, D.A., 2014. Temperature response of photosynthesis  
922 in C<sub>3</sub>, C<sub>4</sub>, and CAM plants: temperature acclimation and temperature adaptation.  
923 Photosynth. Res. 199, 101-117.  
924  
925 Yepes Mayorga, A. 2010. Desenvolvimento e efeito da concentração atmosférica de  
926 CO<sub>2</sub> e da temperatura em plantas juvenis de *Hymenaea courbaril* L., jatobá. PhD  
927 thesis, Universidade de São Paulo, São Paulo.  
928  
929

930 Tables

931 Table 1. ANOVA results for stomatal conductance linear mixed effects model.

932 Temperature and CO<sub>2</sub> refer to treatment effects. Asterisks denote *P* values: \*\*\* *P* <

933 0.0001, \*\* *P* < 0.001, \* *P* < 0.05, • *P* < 0.1, ns not significant.

Model Term	Numerator DF	Denominator DF	F
Intercept	1	551	213.0***
Time	1	551	48.3***
Time <sup>2</sup>	1	551	204.3***
PAR	1	551	28.5***
<i>D</i>	1	551	0.17 <sup>ns</sup>
Temperature	1	28	15.7**
CO <sub>2</sub>	1	28	3.2•
Temperature: <i>D</i>	1	551	6.5*
CO <sub>2</sub> : <i>D</i>	1	551	2.3 <sup>ns</sup>
Temperature:CO <sub>2</sub>	1	28	1.3 <sup>ns</sup>
Temperature:CO <sub>2</sub> : <i>D</i>	1	551	16.7**

934

935 Table 2. ANOVA results for *A-T<sub>L</sub>* linear mixed effects model. CO<sub>2</sub> refers to treatment.

936 Asterisks denote *P* values: \*\*\* *P* < 0.0001, \*\* *P* < 0.001.

Model Term	Numerator DF	Denominator DF	F
Intercept	1	91	421.9***
Leaf Temperature	1	91	66.9***
CO <sub>2</sub>	1	10	14.7*
Leaf Temperature:CO <sub>2</sub>	1	91	11.8**

937

938 Table 3. Parameter estimates of Arrhenius functions of the temperature sensitivity of  
 939  $V_{cmax}$  and  $J_{max}$ . Standard errors are given in brackets. Significance of between  
 940 treatment effects are shown: \*  $P < 0.05$ , •  $P < 0.1$ , ns not significant. Letters denote  
 941 differences between treatments.

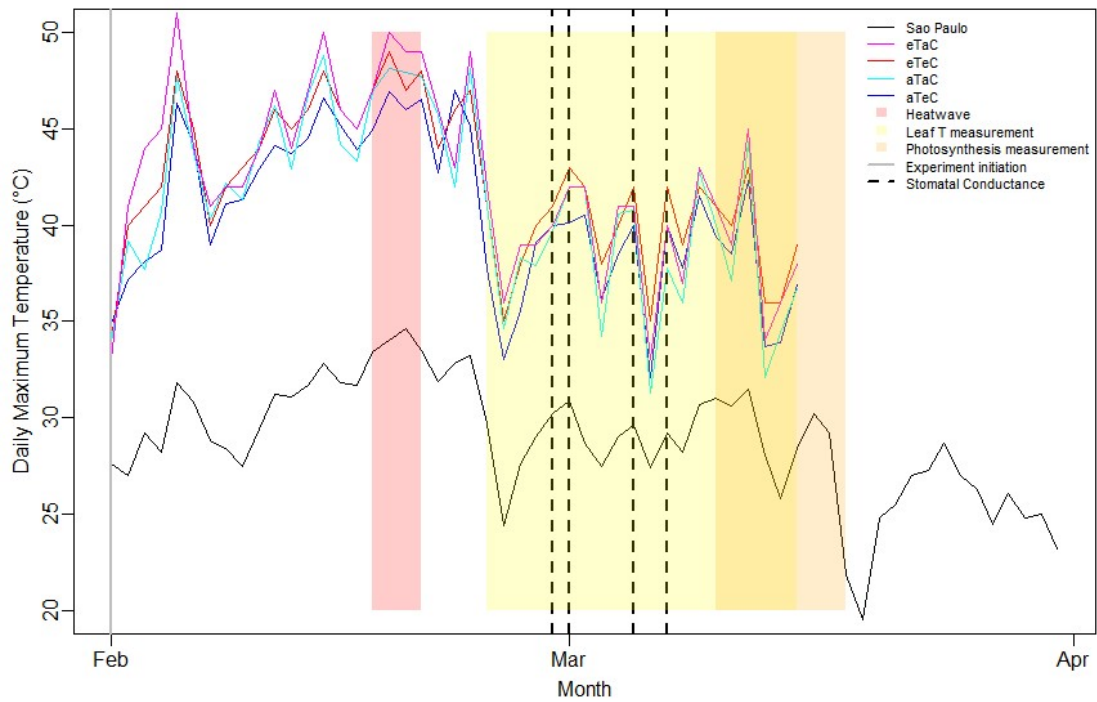
Chamber	$V_{cmax25}$	$E_a (V_{cmax})$	$J_{max25}$	$E_a (J_{max})$
aTaC	13.8 (2.74) AB	81702 (16778) AB	24.95 (1.14)	32187 (4279)
eTaC	14.2 (1.27) A	80644 (7551) A	24.0 (1.84)	27499 (7183)
aTeC	11.0 (1.75) AB	71004 (13689) AB	-	-
eTeC	10.5 (0.26) B	62050 (2171) B	21.8 (3.35)	25840 (14184)
Among Chambers	*	•	ns	ns

942

943

944

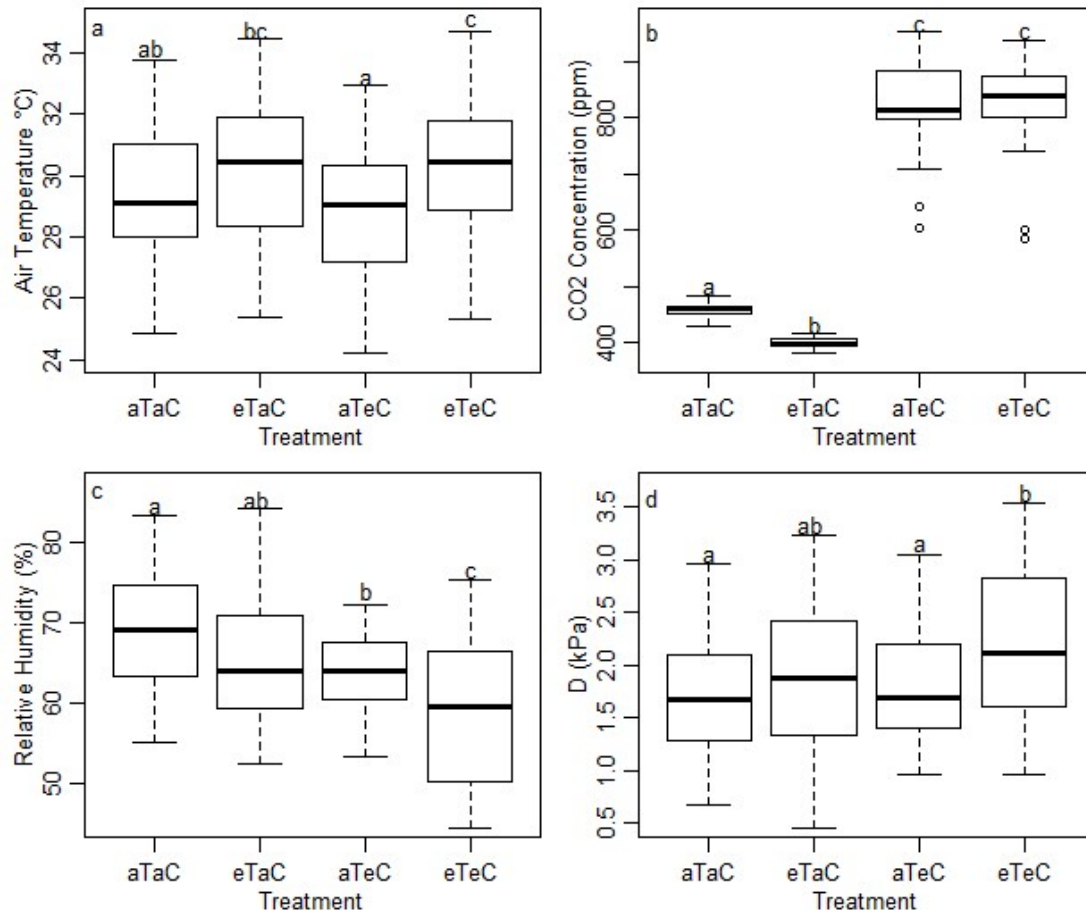
945 Figures



946

947 Figure 1. Time series of daily maximum temperatures in São Paulo (Mirante de  
948 Santana weather station, data from INMET, <http://www.inmet.gov.br/portal/>, accessed  
949 22/05/2018) and in each experimental chamber during the experiment. The  
950 experiment was initiated on 1 Feb 2017. The period classified as a heatwave, periods  
951 of leaf temperature and photosynthesis data collection, and days in which diurnal  
952 cycles of stomatal conductance were performed are shown.

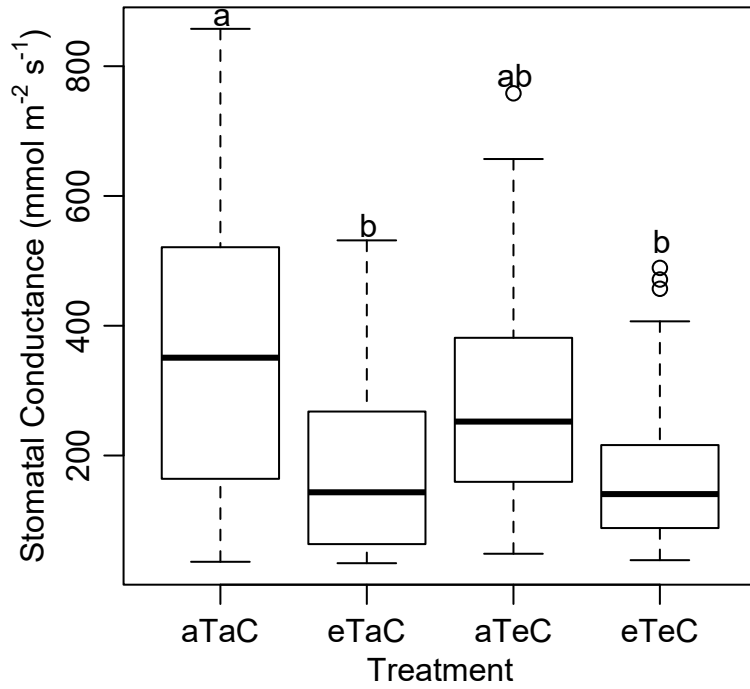
953



954

955 Figure 2. Differences in microclimate variables between chambers a) mean air  
 956 temperature, b) mean CO<sub>2</sub> concentration, c) mean relative humidity, d) mean *D*. Box  
 957 plots show daily averaged values from both the acclimation and measurement periods.  
 958 Treatments: aTaC – ambient temperature and CO<sub>2</sub>, eTaC – elevated temperature and  
 959 ambient CO<sub>2</sub>, aTeC – ambient temperature and elevated CO<sub>2</sub>, eTeC – elevated  
 960 temperature and CO<sub>2</sub>.

961



962

963 Figure 3. Effect of treatment on stomatal conductance where measurements from all

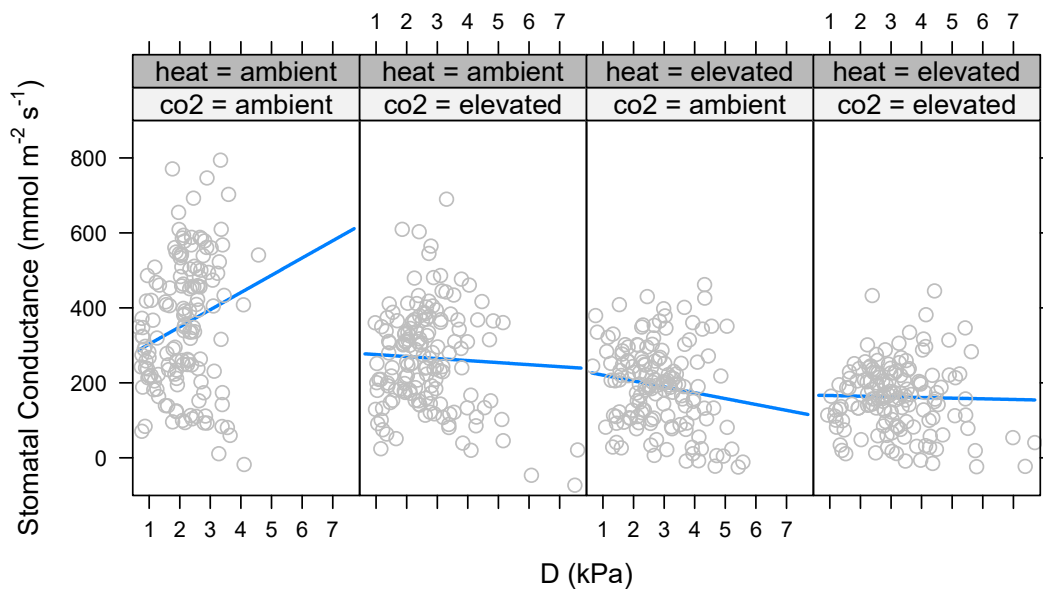
964 times of day are pooled. Treatments: aTaC – ambient temperature and CO<sub>2</sub>, eTaC –

965 elevated temperature and ambient CO<sub>2</sub>, aTeC – ambient temperature and elevated

966 CO<sub>2</sub>, eTeC – elevated temperature and CO<sub>2</sub>.

967

968



969

970 Figure 4. The relationship between  $g_s$  and leaf-to-air  $D$  for each treatment (accounting

971 for time of day ( $t$ , hours) and PAR as fixed effects and leaf as a random factor). Grey

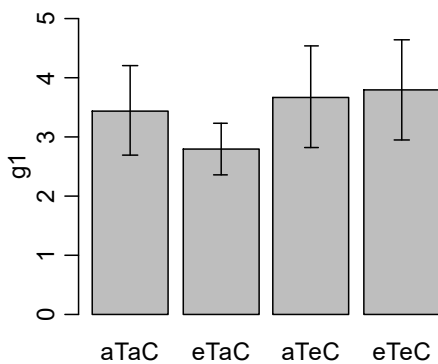
972 points show the partial residuals of the model. Full model equations:  $-1053.2 +$

973  $215.6 \cdot t - 8.6 \cdot t^2 + 0.13 \cdot \text{PAR} + 45.9 \cdot D$  (aTaC);  $-1029.7 + 215.6 \cdot t - 8.6 \cdot t^2 + 0.13 \cdot \text{PAR} -$

974  $7.0 \cdot D$  (aTeC);  $-1074.1 + 215.6 \cdot t - 8.6 \cdot t^2 + 0.13 \cdot \text{PAR} - 17.3 \cdot D$  (eTaC);  $-1142.5 +$

975  $215.6 \cdot t - 8.6 \cdot t^2 + 0.13 \cdot \text{PAR} - 2.6 \cdot D$  (eTeC).

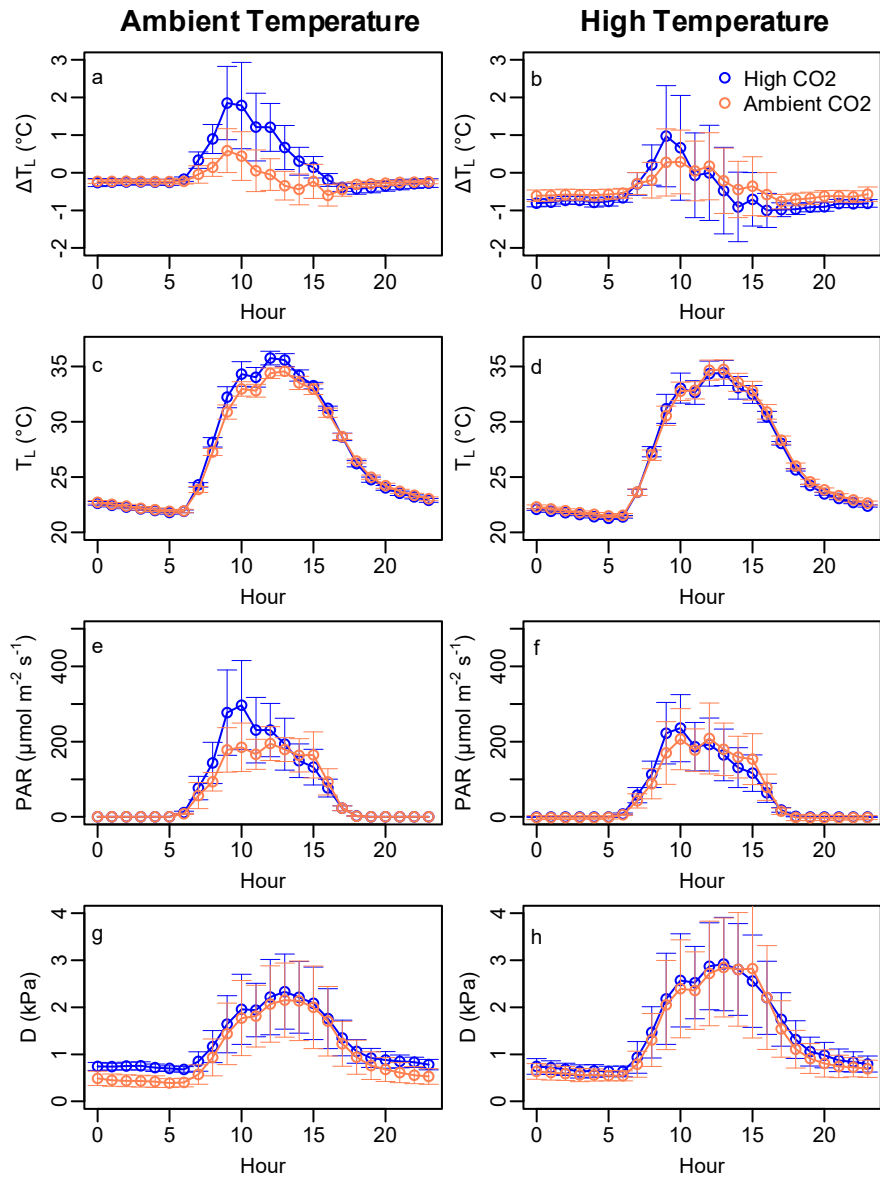
976



977

978 Figure 5. Comparison of the  $g_1$  stomatal conductance parameter (unitless) between

979 chambers. Bars show the mean value and error bars the standard deviation.

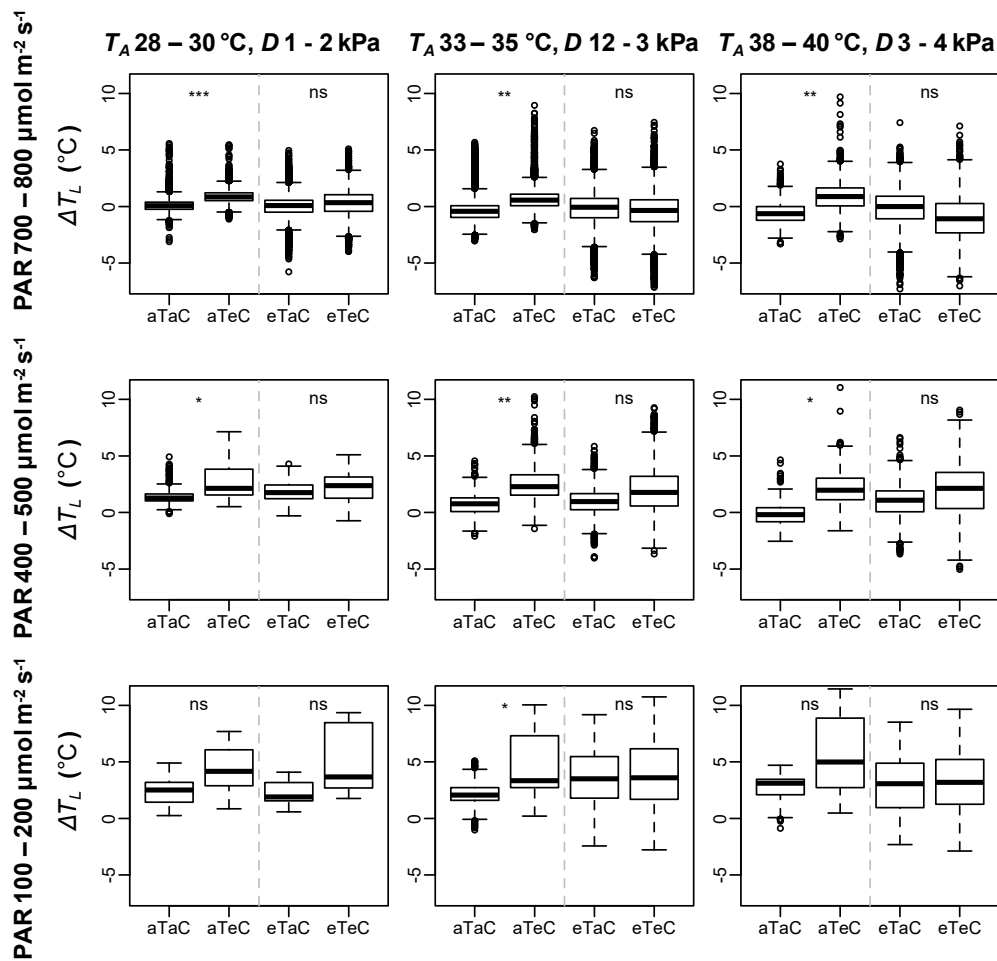


980

981 Figure 6. Diurnal cycles of leaf-to-air temperature difference (a,b), leaf temperature

982 (c,d), PAR (e,f),  $D$  (g,h), for chambers with ambient air temperature (a,c,e,g) and

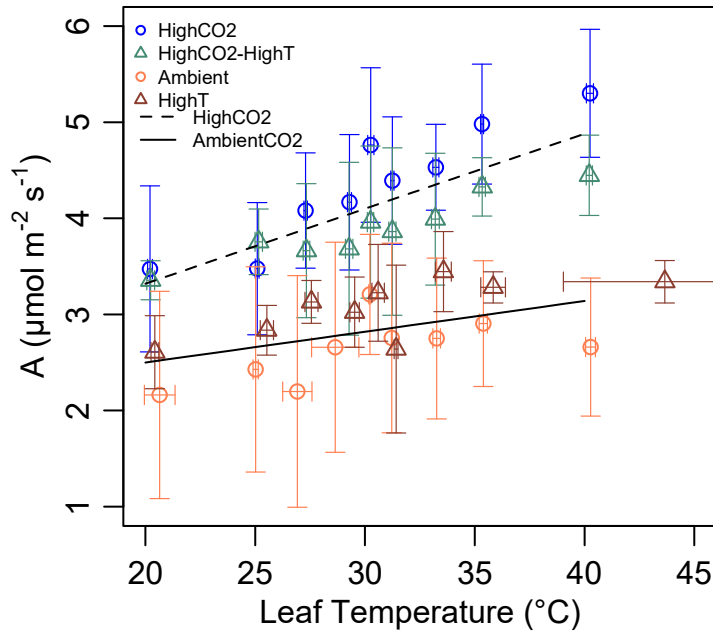
983 elevated temperatures (b,d,f,h).



984

985 Figure 7. Leaf to air temperature differences for each treatment under a range of  
 986 microclimate conditions. Contrasts are made between aC and eC under ambient the  
 987 temperature treatment, and between aC and eC under the elevated temperature  
 988 treatment, using mixed effects models with leaf as a random factor. Data is from  $\Delta T_L$   
 989 measurements at 10 s temporal resolution subsetted for specific chamber air  
 990 temperature ( $T_A$ ) and  $D$  conditions, and leaf surface PAR conditions. Asterisks denote  
 991  $P$  values: \*\*\*  $P < 0.0001$ , \*\*  $P < 0.001$ , \*  $P < 0.05$ , ns not significant.

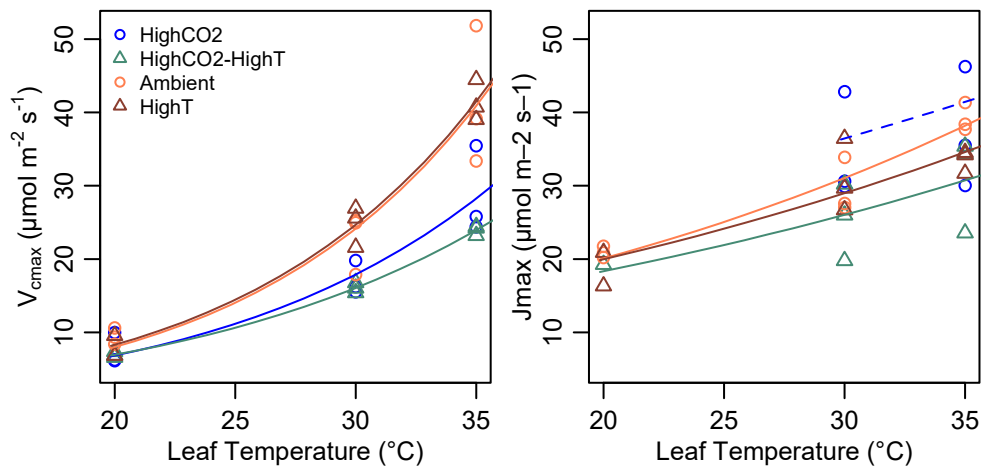
992



993

994 Figure 8. Temperature response of net photosynthesis. Under high CO<sub>2</sub> net  
 995 photosynthesis is higher and the temperature response is steeper. For ambient CO<sub>2</sub>  $A$   
 996  $= 1.86 + 0.032 \cdot T_L$ ; for elevated CO<sub>2</sub>  $A = 1.75 + 0.078 \cdot T_L$ .

997



998

999 Figure 9. Temperature response of  $V_{max}$  and  $J_{max}$  fit with Arrhenius functions. For  
 1000  $J_{max}$  in the high CO<sub>2</sub> treatment no values at 20 °C were obtainable. Equation  
 1001 parameters are given in Table 3.